

## **Application of Measured Value Approach's and MATLAB Programme in Prediction of Drillship Station Keeping Status in various Sea State**

**Musa Ozozoyin Ebenezer<sup>1</sup>, Nwaoha Thaddeus Chidiebere<sup>2</sup>, Agbakwuru Jasper<sup>3</sup>**  
<sup>1,2,3</sup>Department of Marine Engineering, Federal University of Petroleum Resources, Effurun, Nigeria  
Corresponding author (s): [musaebenezer@gmail.com](mailto:musaebenezer@gmail.com)

### **ABSTRACT**

The study was undertaken to predict the seakeeping ability of a drillship at sea using a set of measured data retrieved from the ship. The study applied measured techniques and MATLAB program to predict the station keeping ability of a drillship with emphasis on wave estimate, true heading angle and generated wave motions. Findings from the study with respect to the research methodologies revealed disparities in wave height estimate, true heading angle estimate and regenerated wave in various ship motions using the measured value approach. Likewise, the drill ship speeds by transfer functions showed huge difference between the encounter domain and absolute domain as the drillship speed influences the heading accuracy of the ship, thus, resulting in various ship motions and degrees which alter the optimal station keeping ability of the drillship. In addition, the accuracy of the estimation of the peak period was revealed to be relatively high while the accuracy for the mean period and zero-up crossing period deviated from the true value. In general, the measured values were not reflections of the true heading state of a drillship, as there is need for incorporating more modified systems and simulations to better predict the ship keeping ability under various wave impacts at sea.

**Keywords:** Drill-ship; Matlab, Wave Estimate; Wave Motions.

### **1. Introduction**

Ships are built for numerous operations in marine environment, especially at sea. In order to accomplish its basic mission, a ship must possess certain characteristics; it must float in stable upright position, move with sufficient speed, and be able to maneuver at sea and in restricted waters, and be strong enough to overcome the rigors of heavy weather and wave impact. To design a ship with these features, the naval architects must understand the dynamics of ships while applying the rules and regulations of the International Association of Classification Societies (IACS). The operation of marine vessels is in environment that is rich in winds and waves (Marion et al., 2024).

Due to the numerous numbers of ships of various sizes and applications, there is an increasing complexity in the maritime navigation environment which threatens maritime safety (Daiyong et al, 2024). Chen et al, (2023) stated that various abnormal ship behaviour increases the risk of collisions, groundings and reef encounters. Hence, predicting ship behaviour in various sea state will minimize navigational risks. Ship motion is influenced by maritime environment and

ship maneuverability. Although, it was opined by Elipoulou et al., (2023) that 80-85% of accidents in the last two years are attributed to human faults. Optimal prediction of ship motion can help to minimize energy consumption, voyages and greenhouse gas emissions. Seakeeping refers to the performance and response of a ship in various sea going conditions. The ability of a Marine craft to maintain seakeeping ability is known as seaworthiness (Subhdeep, 2022). However, ship parameters such as structural integrity, propulsive efficiency influences the design spiral of a ship. Seakeeping of marine craft investigation is an interesting area of investigation due to various factors, such as maximum speed in a seaway, route optimization, structural design of ship, habitation and ship safety (Volker, 2012). Model tests, full scale measurement on ship at sea and computations in time and statistical domain are some of the tools to predict seakeeping of ship. However, there tends to be some challenges in the application of the seakeeping prediction tools owing to natural seaway such as superposition of harmonic waves and inclusion of harmonic waves to a total reaction superposition.

## **2. Review of Literature**

Karol and Artur (2020) examine the determination of seakeeping performance for a case study vessel using the strip theory method. Findings from the study revealed that the seakeeping performance is greatly affected by the hull shape and its process of sectioning. Zu et al., (2024) assessed the criteria for seakeeping ability. Results from the findings showed that vessel survivability depends on the hull intact stability and structural design. Furthermore, the study revealed that it is necessary to develop seakeeping criteria for certain vessel types. To address the issues of operability, NATO (2018) developed and applied NATO criteria specifically for naval warfare which include combat and auxiliary ships using mission-oriented approach with emphasis on safety. Results from the analysis was positive as provided a framework on crew's effectiveness, naval air operations, towed system and damage control. In order to minimize occupational accidents and limited safe operation in ship, Tello et al. (2011) establish design rules for fishing vessels less than 24 m in length using different hull forms in sea states. Findings from the study showed that the design criteria provided decision support system to aid awareness during fishing operations. Similarly, the prediction of sea keeping in the early stage of conventional mono-hull vessels design using artificial neural network (ANN) was investigated by Romero-Tello et al. (2023). The proposed methodology was applied to deduce the predictive algorithm using the database of ships for training the ANN. The data was generated using frequency domain sea keeping code depending on the boundary element method. Findings from the study gave comparison between the boundary element method and ANN which were found to be satisfactory. To improve seakeeping evaluation, De-Alwis et al. (2020), developed and recommend revision methods to evaluate the musculoskeletal health implications of shock and vibration from exposure to vessel motion. The study provided information's for buoy-tending, fire-fighting, crane, search and rescue and hydrographic survey.

## **3. Methodology**

This study employed the use of primary and secondary data to establish relevant information that relates to the purpose of the study. This paper employs the use of MATLAB programs and measured values techniques to obtain results for estimated wave height at specified speed, optimum heading at minimum, wave spectrum and transfer function utilizing closed form expression. The data produce from the MATLAB program was compare to the estimated true heading in order to deduce the mean and standard deviation error.

Important data in the MATLAB programs such as the vessel motions and the transfer functions formed part of the study as the vessel motions can either be simulated or real measured values

over time from an in-service vessel which forms a serious challenge in effective seakeeping ability or performance for a ship. The important of these parameters is that they are organized according to Table. 1 where time is denoted in seconds. Also, the actual motions are usually six possible motions, however, for simplification and major concern, heave, roll and pitch was considered where heave is in meters and roll and pitch are in degrees.

Table. 1: Schematic structure of the vessel motions data that is to be used in the MATLAB® programs.

Time (sec)	Heave (m)	Roll (deg)	Pitch (deg)
$t_1$	$z_1$	$\emptyset_1$	$\theta_1$
$t_2$	$z_2$	$\emptyset_2$	$\theta_2$
$t_3$	$z_3$	$\emptyset_3$	$\theta_3$
.	.	.	.
.	.	.	.
.	.	.	.
$t_N$	$z_N$	$\emptyset_N$	$\theta_N$

To enable an investigation at various vessel speeds, several transfer functions need to be calculated corresponding to each condition and each case has to follow the structure described in Table 2 where it should be an even increment step size of the heading  $\chi \in [0, 360]$  and the structure should start with following seas.

Table 2: Schematic structure of the wave elevation data that is to be used in the MATLAB programs.

Time (sec)	Wave elevation
$t_1$	$\zeta_1$
$t_2$	$\zeta_2$
$t_3$	$\zeta_3$
.	.
.	.
.	.
$t_N$	$\zeta_N$

In cooperation with DNV GL vessel used for this study, the data provided included the motions of the vessel, the transfer functions for heave, roll and pitch along with the directional wave spectrum measured with the system Miros Wavex . The information gathered from the vessel was first of all re-structured according to the format described in Table1. After which, the transfer functions were only available for specific vessel speeds and in a first stage, motion time periods were selected so the speed of the vessel at the time of measurement were of the same speed of the available transfer functions. This task requires extensive work to first find time periods where the heading and speed was fairly constant and then transform the data into the correct structure and then run the estimation procedure.

#### 4. Results and Discussion

Figure 1-7 shows the generated results for various estimated wave height, wave spectrum and responses in the encounter domain while Table 3-8 reveals the corresponding significant wave estimates errors using the measured values approach.

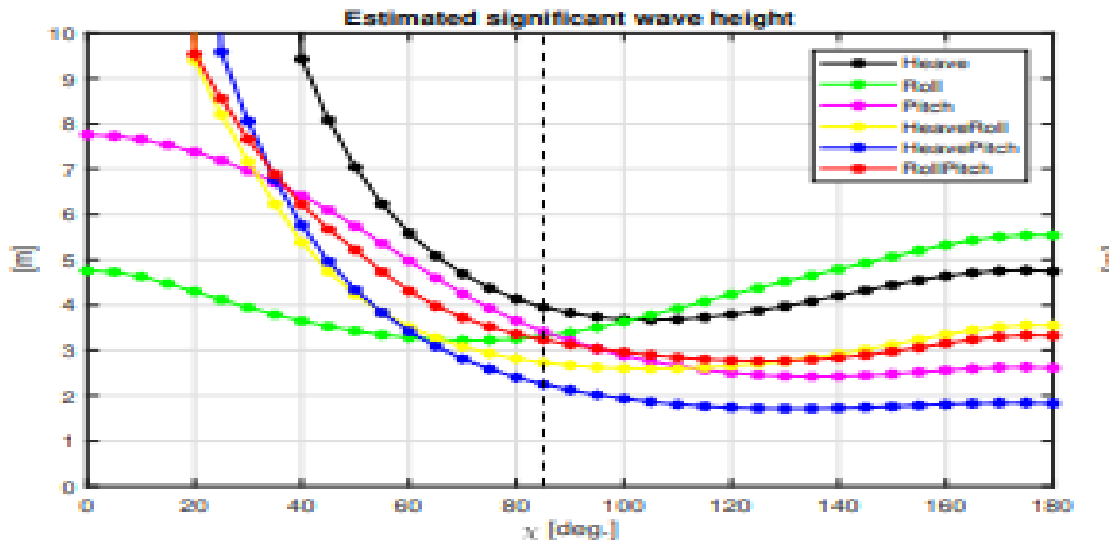


**Fig. 1:** Estimated angle is 85 deg. and the true angle is 90 deg.

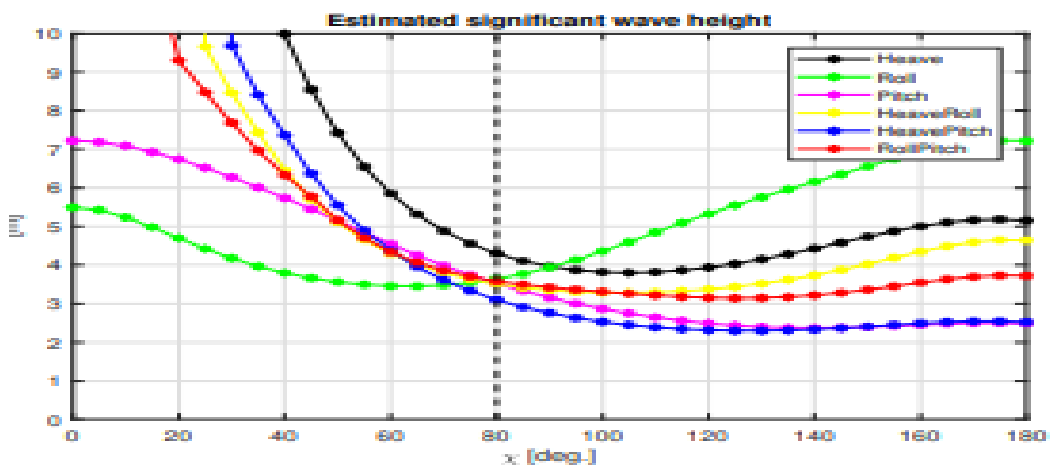


**Fig. 2:** Estimated angle is 80 deg. and the true angle is 270 deg which is the symmetry angle to 90 deg

The calculated estimation of the wave spectrum based on only the absolute values of the transfer functions, i.e. only considering the spectra of  $\chi \in [0, 180]$  deg.  $\beta_0$  is chosen based on the angle where the lowest variation occurs which is indicated by the vertical dotted line, the significant wave height is taken as the average value of the responses at the same angle.

The information retrieved from the first estimate, which can be seen in Fig. 1, is not sufficient alone since it only shows the heading on the spectrum of  $\chi \in [0, 180]$  and the intention is to calculate on the full compass,  $\chi \in [0, 360]$  deg. To achieve this, the imaginary parts of the transfer functions must be added and considered in the estimation. Two examples of the results of this practice is shown in Fig. 3 were the actual wave heading estimate is found were the blue line, named 'Total', takes its minimum value. This secondary heading estimate is  $\beta_2 \in [0, 360]$  deg.

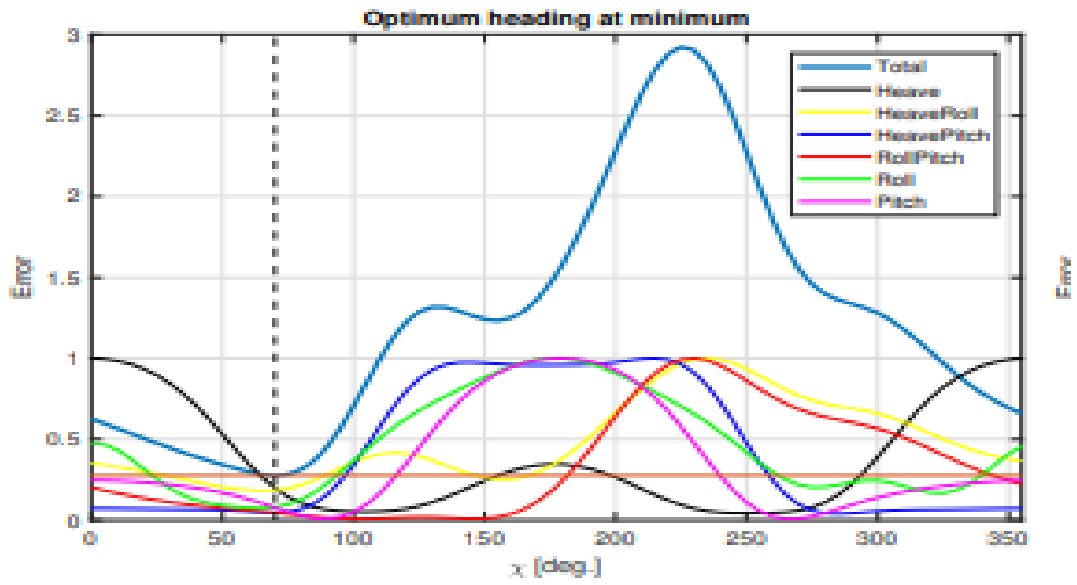


Fig.3: Estimated angle is 70 deg. and the true angle is 90 deg.

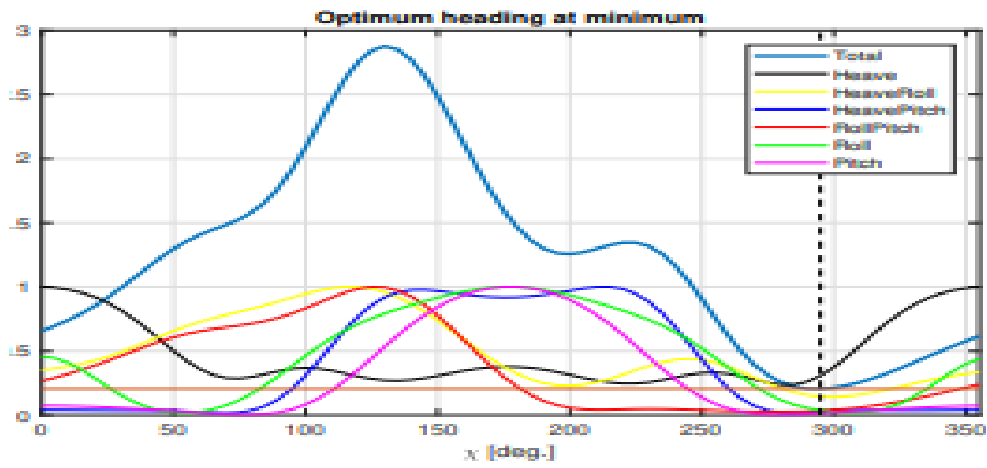
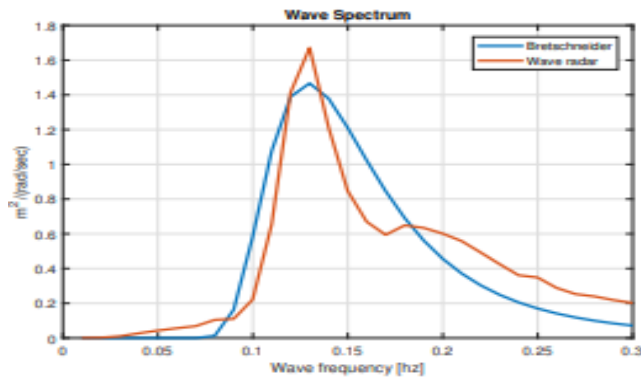
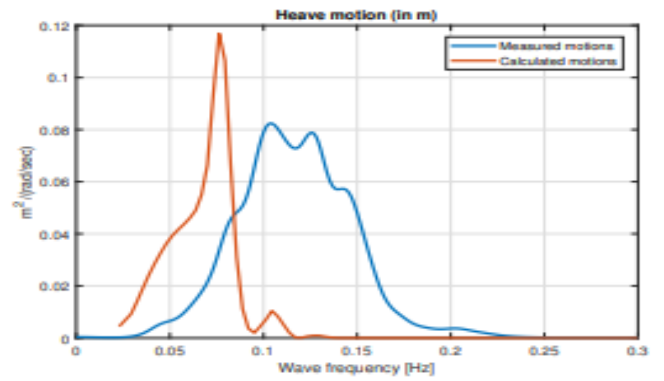


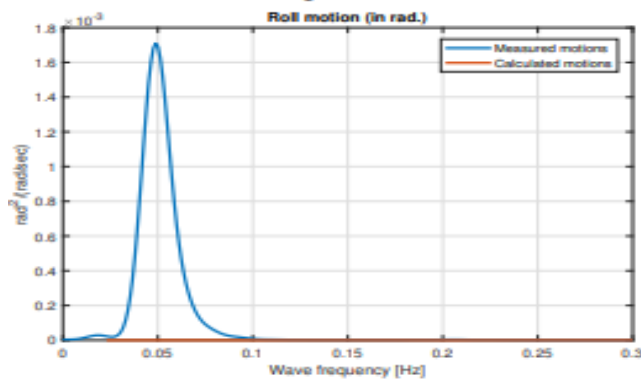
Fig. 4: Estimated angle is 285 deg. and the true angle is 270 deg



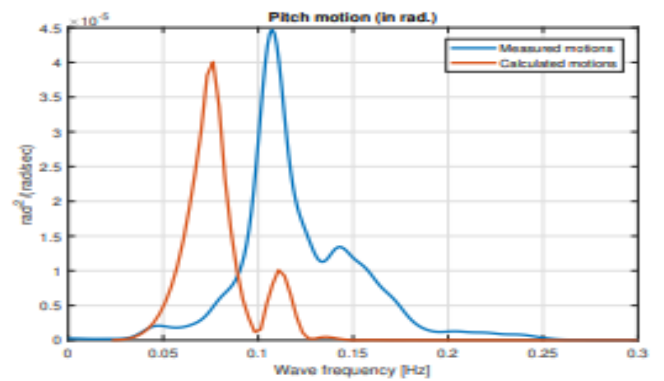
(a) Comparison of the wave spectrum and a Bretschneider wave spectrum with the same wave parameters.



(b) Comparison of the heave motions based on measured values and calculated based on the transfer function.



(c) Comparison of the roll motion based on measured values and calculated based on the transfer function.



(d) Comparison of the pitch motion based on measured values and calculated based on the transfer function.

Fig. 5: Re-generated vessel motions based on the transfer functions in combination of the directional wave spectrum.

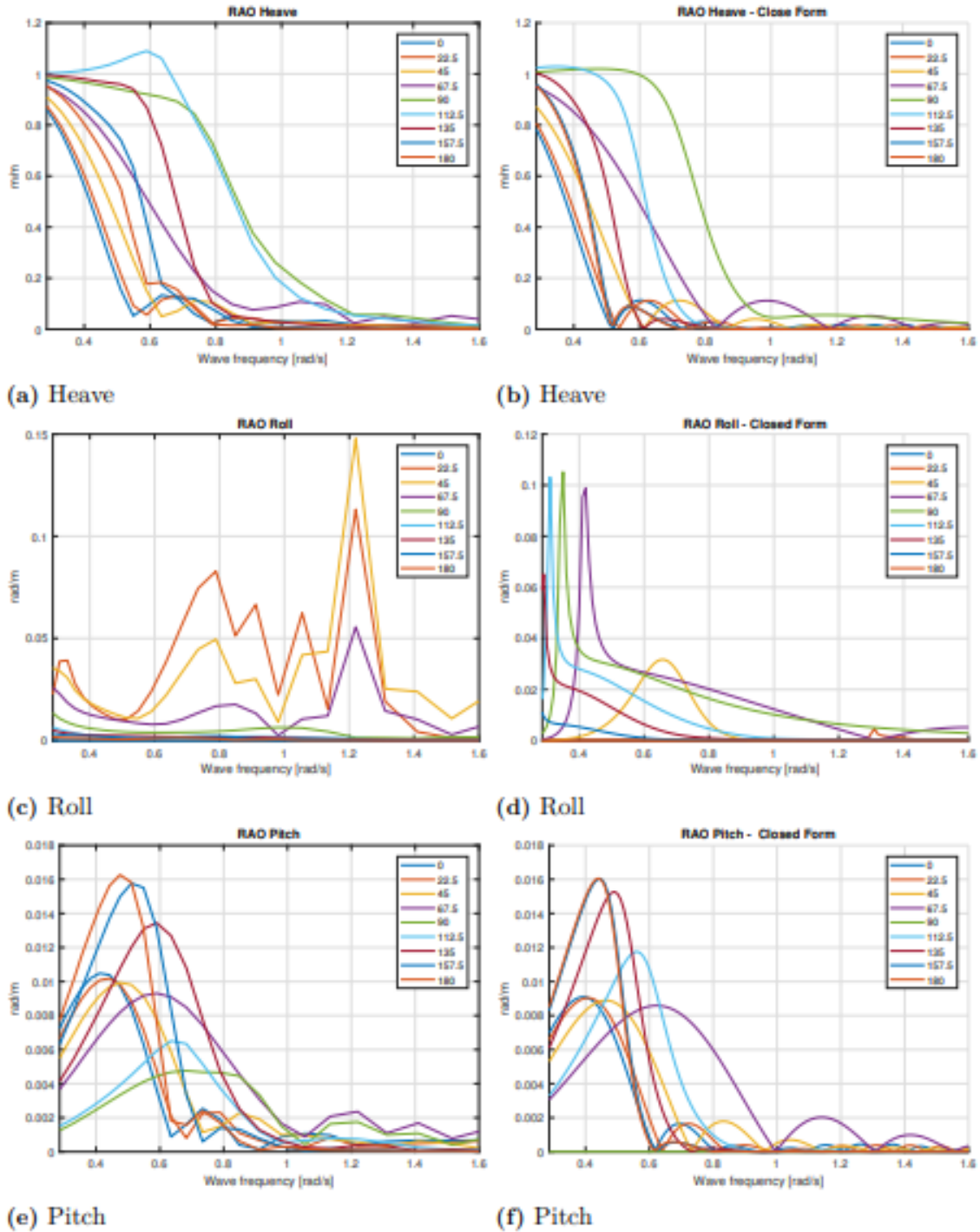
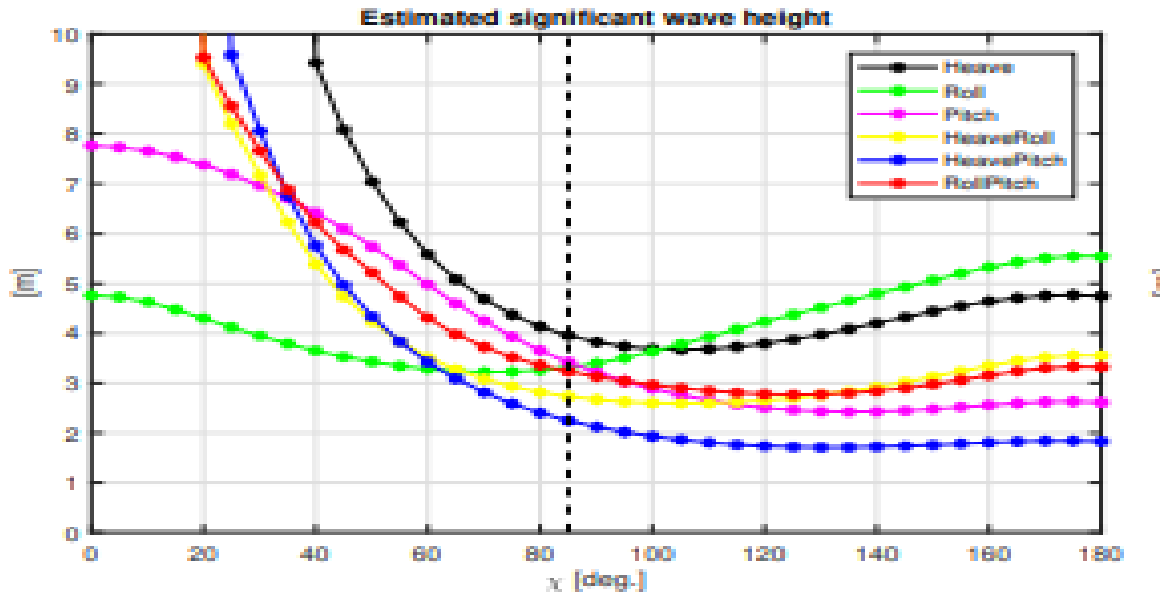
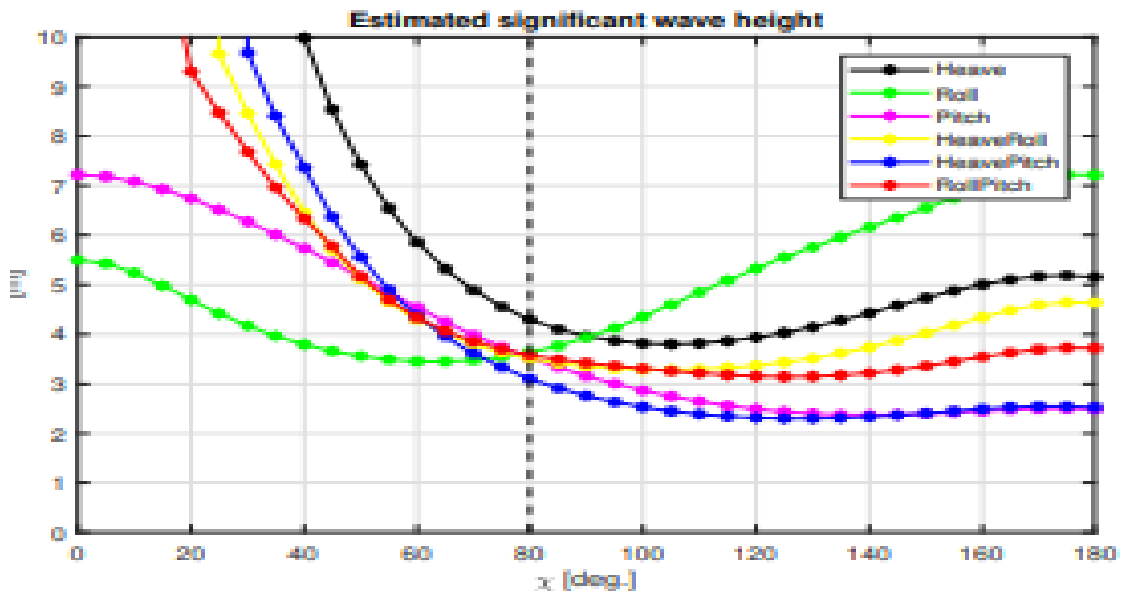


Fig. 6a-f: Comparison between the transfer functions obtained from the software Sesam with transfer functions calculated based on the closed form expressions by Jensen et al. (2004). On the left side is the software calculated functions, on the right side is the closed form expressions functions.



**Fig. 7:** Estimated angle is 85 deg. and the true angle is 90 deg.



**Fig. 8:** Estimated angle is 80 deg. and the true angle is 270 deg which is the symmetry angle to 90 deg

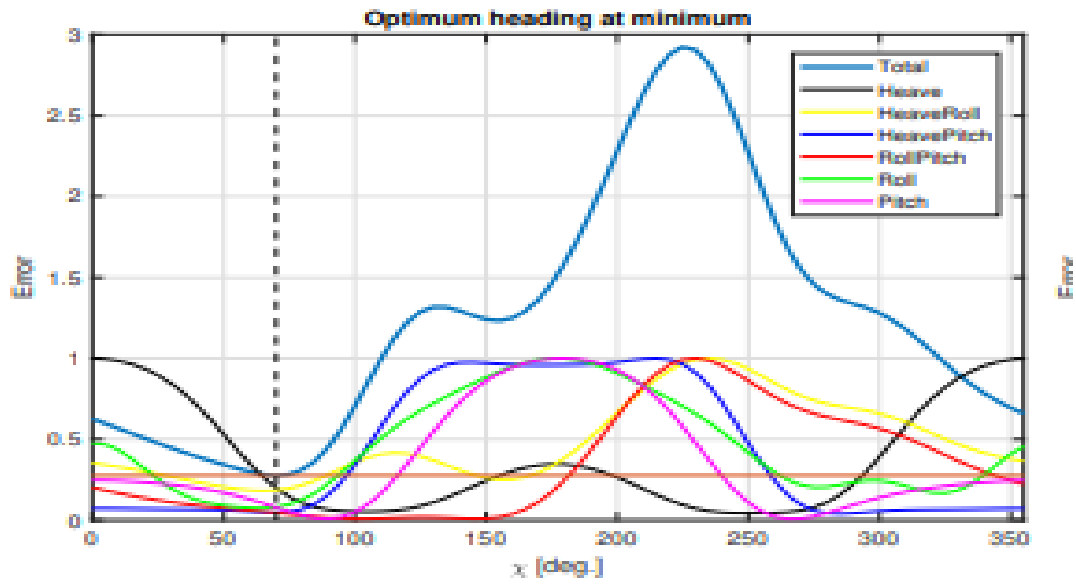


Fig. 9: Estimated angle is 70 deg. and the true angle is 90 deg.

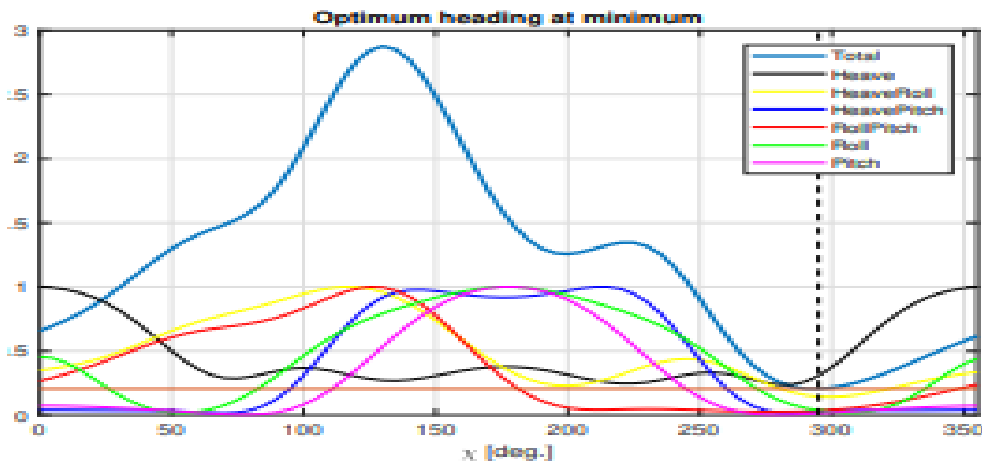


Fig. 10: Estimated angle is 285 deg. and the true angle is 270 deg

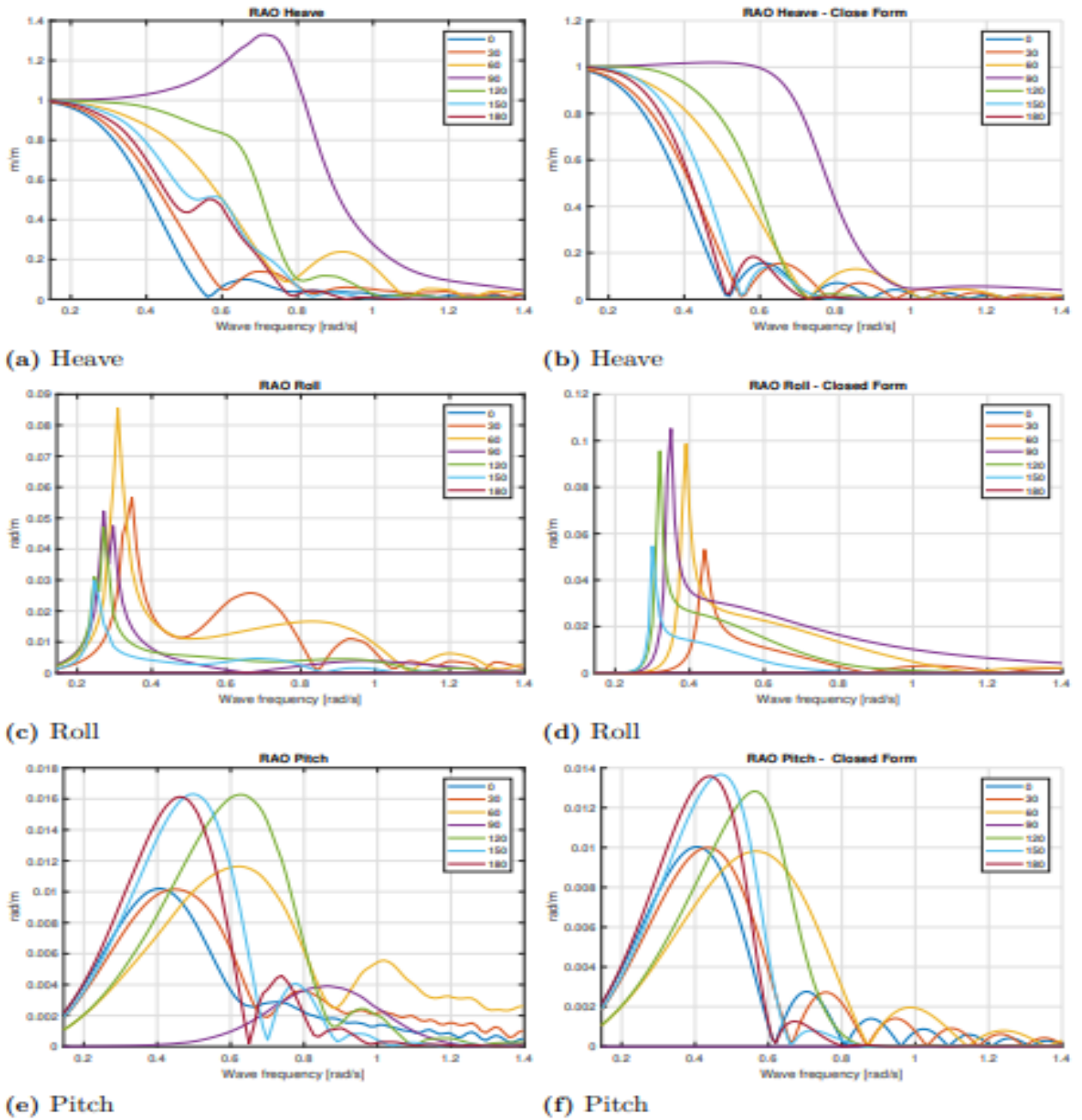


Fig. 11: Comparison between the transfer functions obtained directly from DNV GL with transfer functions calculated based on the closed form expressions

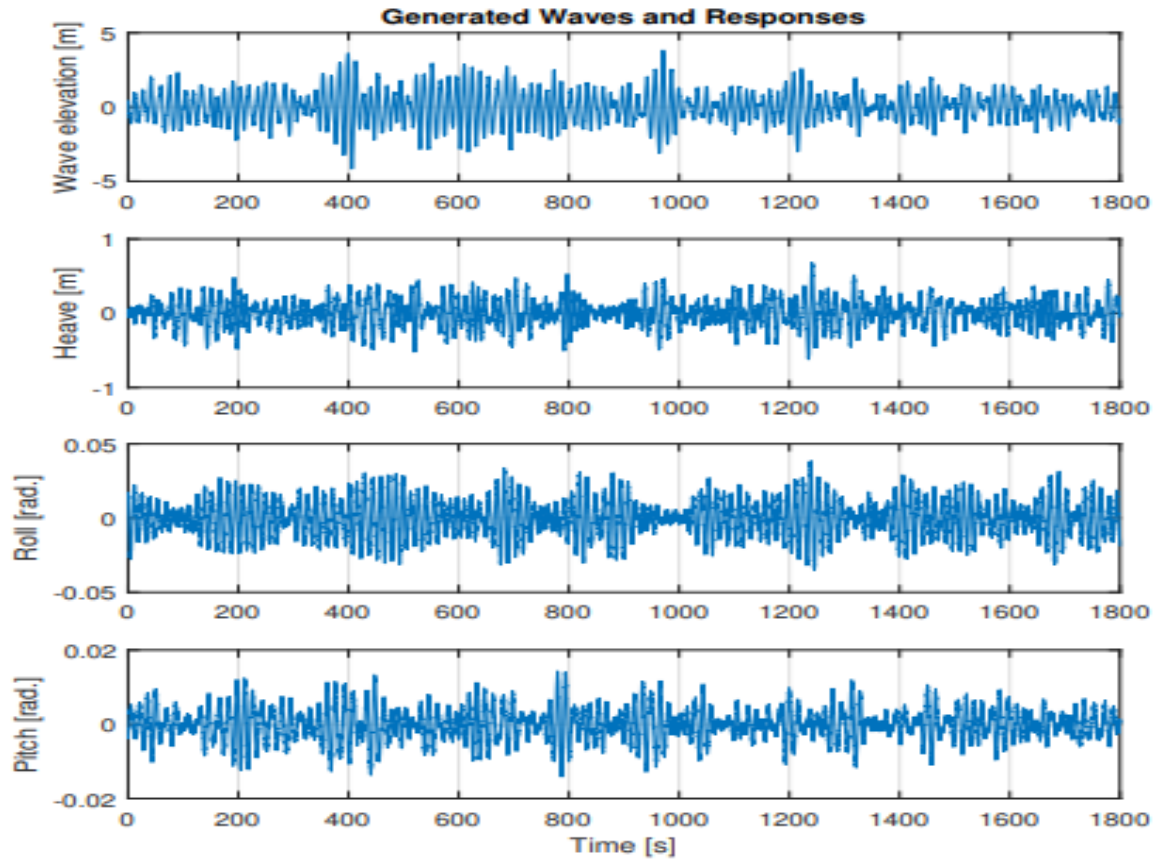
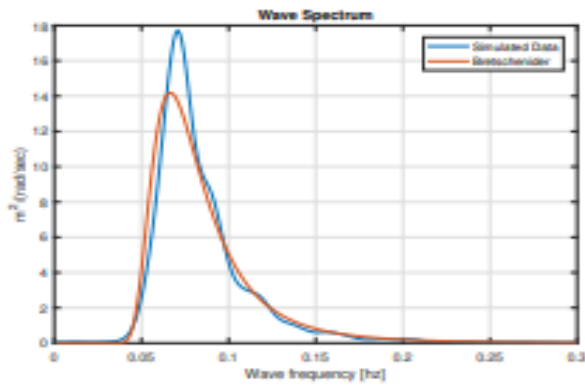
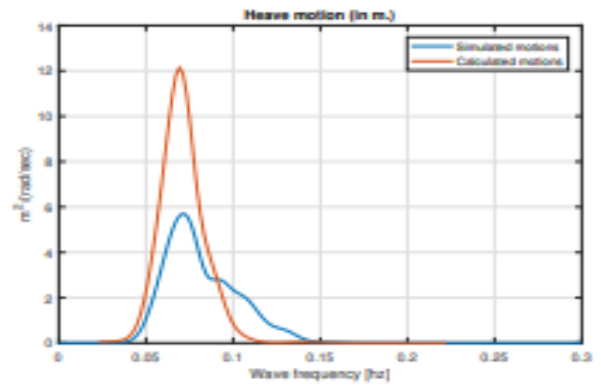


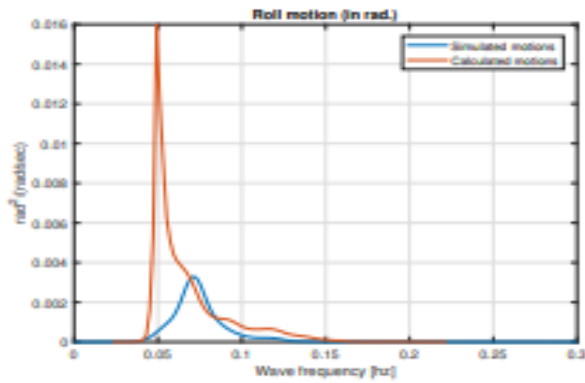
Fig. 12: Simulated vessel motions together with the wave elevation. The top plot is the wave elevation in meters over a half hour period, second plot is the heave motion in meters over the same half hour period, third and fourth plot is the roll and pitch motion respectively in radians over the same half hour period.



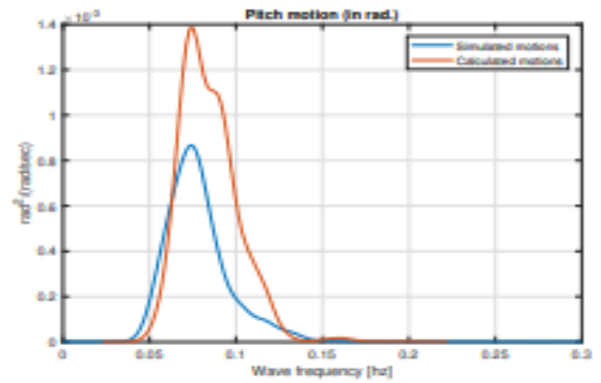
(a) Comparison of the simulated wave spectrum and a Bretschneider wave spectrum with the same wave parameters.



(b) Comparison of the heave motions based on simulated values and calculated based on the transfer function.



(c) Comparison of the roll motion based on simulated values and calculated based on the transfer function.



(d) Comparison of the pitch motion based on simulated values and calculated based on the transfer function.

Fig. 13: Re-generated vessel motions based on the transfer functions in combination with the simulated wave spectrum.

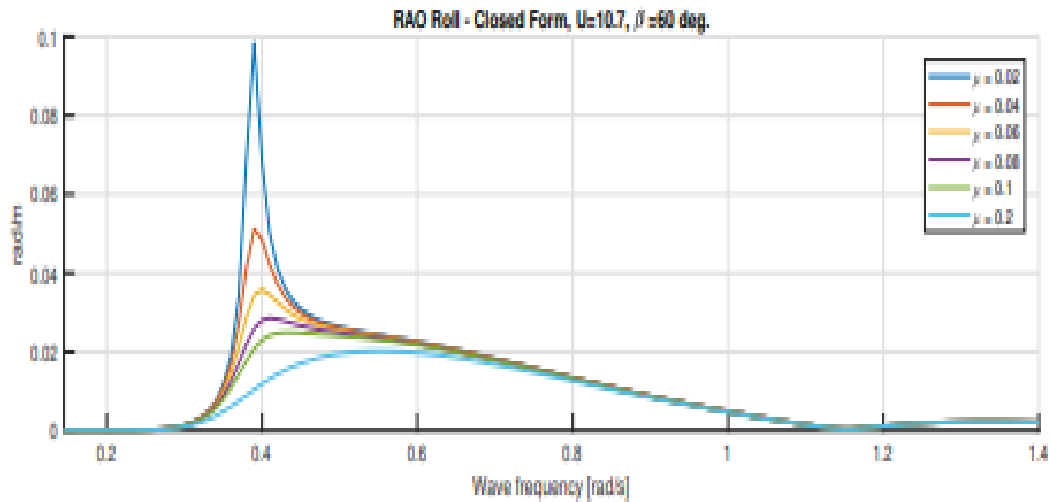


Fig. 14: The effect of different added damping on the roll transfer functions

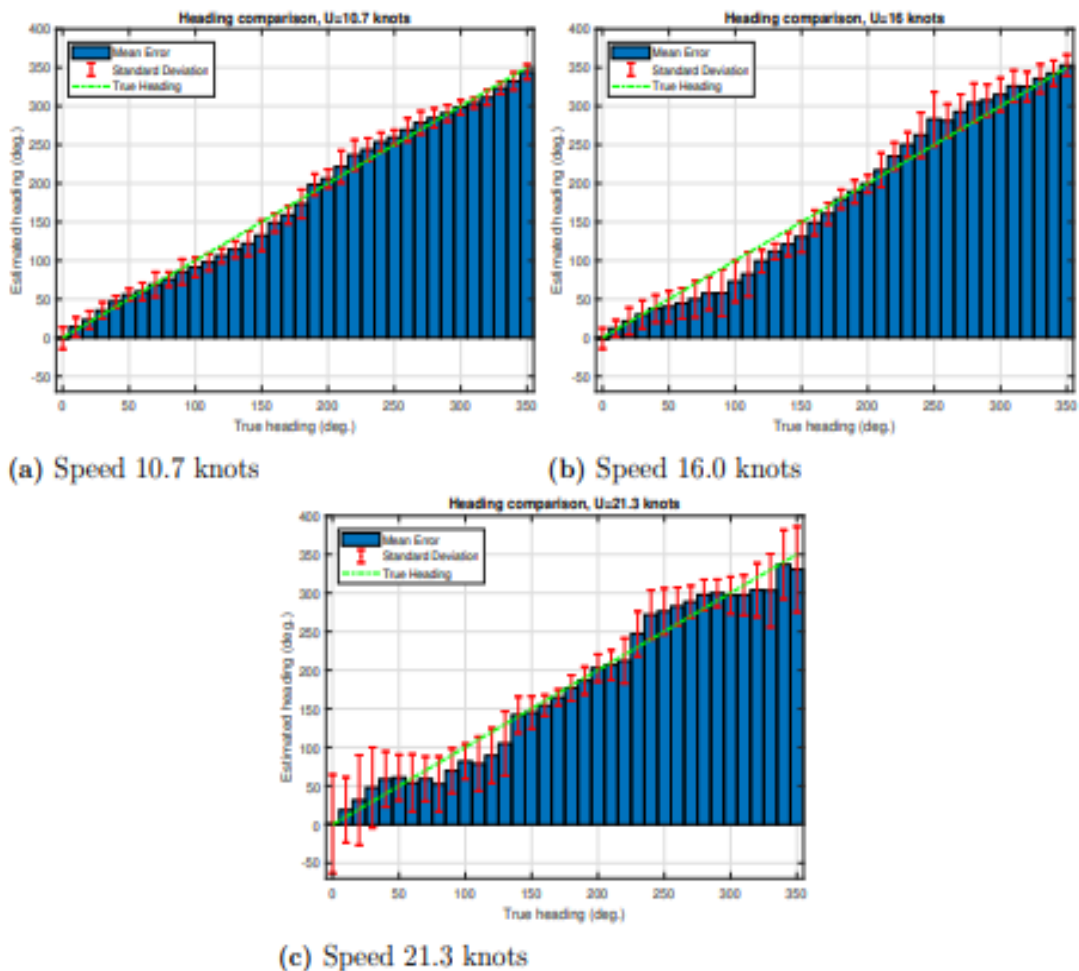


Fig. 15: Comparison of the estimated heading with the true heading at 10.7, 16.0 and 21.3 knot

The blue bar represents the mean value of the heading estimate, the red line represents the standard deviation of each heading estimate and the green dotted line represent the optimal case where the estimated heading is the same as the true heading

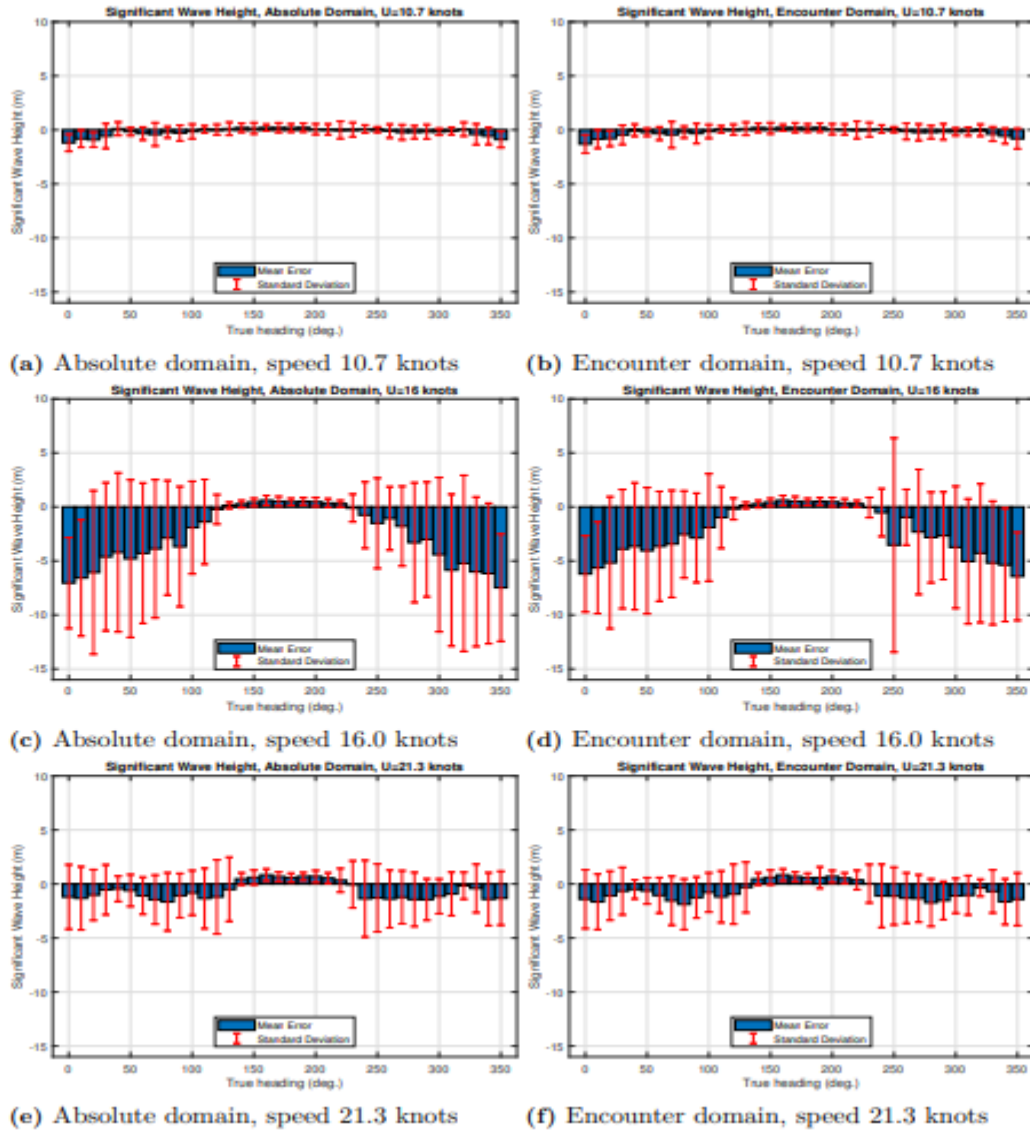


Fig.16: Comparison of the estimated significant wave height with the true significant wave height.

To the left, the absolute domain comparison is displayed while on the right side the encounter domain comparison is shown. The blue bars represent the mean error between the true and estimated height for each true heading and the red line represent the standard deviation of the error values.

Table 3: The heading estimate errors per speed using the original estimation procedure.

Speed (knot)	Mean absolute error (deg)	Standard deviation of the error	Correctly chosen heading (%)
<b>10.7</b>	<b>14.6</b>	<b>12.3</b>	<b>66.9</b>
<b>16.0</b>	<b>21.9</b>	<b>24.8</b>	<b>54.6</b>
<b>21.3</b>	<b>25.9</b>	<b>22.0</b>	<b>37.9</b>

Table 4: The significant wave height estimates errors per speed using the original estimation procedure.

Speed (knot)	Mean absolute error	Standard deviation
<b>10.7</b>	<b>1.14</b>	<b>2.25</b>
<b>16.0</b>	<b>6.52</b>	<b>13.20</b>
<b>21.3</b>	<b>4.23</b>	<b>10.27</b>

Similarly, the error of the significant wave height is shown in Table 8 for the same set of time series.

Table 5: The improved heading estimate errors per speed using the developed rules in Algorithm 2.

Speed (knot)	Mean absolute error (deg)	Standard deviation of the error	Correctly chosen heading (%)
10.7	7.6 (14.6)	10.4 (12.3)	78.1 (66.9)
16.0	12.7 (21.9)	25.1 (24.8)	86.9 (54.6)
21.3	7.5 (25.9)	14.9 (22.0)	93.4 (37.9)

Table 6: Summarized results for the heading estimate including the mean error for all “true” headings and the standard deviation for the same spectra.

Speed (knots)	Mean error (deg)	Standard deviation of the Error
10.7	1.57	20.79
16.0	0.66	26.23
21.3	1.95	37.48
All	1.39	28.99

Table 7: Summarized results for the heading estimate including the absolute mean error for all “true” headings and the standard deviation for the same spectra.

Speed (knots)	Mean error (deg)	Standard deviation of the Error
10.7	12.57	16.95
16.0	18.26	18.84
21.3	23.70	29.10
All	18.02	22.75

Table 8. Summarized results for the significant wave height estimate including the mean error for all headings and the standard deviation for the same spectra.

Speed (knots)	Mean Error (m)	Standard deviation of the error
<b>Encounter Domain</b>		
10.7	-0.18	0.72
16.0	-2.31	4.78
21.3	-0.67	2.04
All	-1.05	3.16
<b>Absolute domain</b>		
10.7	- 0.17	0.71
16.0	- 2.61	5.43
21.3	- 0.62	2.26
All	-1.13	3.58

The main results of the sea state estimation procedure proposed by Nielsen et al. (2018) are the wave parameters; significant wave height, ( $H_s$ ), peak period, ( $T_p$ ), mean period, ( $T_m$ ), zero-up crossing period, ( $T_z$ ), and wave heading, ( $\beta$ ). The estimation results can either be presented in the encounter domain or the absolute domain depending on what application the estimation is intended for. Furthermore, the transformation between different domains is somewhat

cumbersome and can in certain cases introduce errors in the estimate. The Doppler effect as well as the fact that the heading estimate is very important for the periods to be correctly transformed from one domain to the other. Therefore, the estimates both before and after the transformation will be presented ensuring the best coverage possible. The results will be presented sorted by parameters were encounter- and absolute domain will be side by side for the specific speed cases which are; 10.7, 16.0 and 21.3 knots. The results will be presented in the same order as it was calculated, starting with heading estimate, significant wave height and then the periods. In Fig. 1, the mean heading estimate for each true heading is presented together with the standard deviation. The green line represents the “correct” estimation which is the goal of the procedure.

In Fig. 2 the mean error of the estimated significant wave height is presented, where the error definition indicated that a negative error indicates that the estimated value is higher than the true value. The peak period is presented in Fig. 3, the zero-up crossing period in Fig. 4 and mean period in Fig. 5. Note that all sub-figures in the same figure have the same y-axis limits. The results are selection of data indicating the errors for different speeds of the different 5 main wave parameter.

The resulting heading estimate using the created rules in Algorithm 2 performs well. It is possible to distinguish trend in Fig. 1 that the higher the speed is, the lower the accuracy of the estimate is. The figures indicate that the highest accuracy is found in head seas, 180 deg., and in following seas, meaning close to 0 or 360 deg. The same trend cannot be seen in Table 2 since it takes the whole mean value, and the procedure underestimates the heading in the spectra 0-180 deg. while overestimating the heading in the spectra 180-360 deg. which in turn eliminates each other creating a very low mean error. Thereby, it can be of better interest to investigate the absolute mean error that is presented in Table 2.

The resulting heading estimate using the created rules in Algorithm 2 performs well. It is possible to distinguish trend in Fig. 1 that the higher the speed, the lower the accuracy of the estimate. The figures indicate that the highest accuracy is found in head seas, 180 deg., and in following seas, meaning close to 0 or 360 deg. The same trend cannot be seen in Table 1 since it takes the whole mean value, and as seen in e.g. Fig. .1 the procedure underestimates the heading in the spectra 0-180 deg. while overestimating the heading in the spectra 180-360 deg. which in turn eliminates each other creating a very low mean error. Thereby, it can be of better interest to investigate the absolute mean error that is presented in Table 2.

By using the information about the wave angle and the vessel speed it is possible to know the characteristics to calculate the absolute domain spectrum by introducing the Doppler effect. After doing so, all the information wanted is estimated, which implies values on the significant wave height, the wave encounter angle and the periods. The calculated estimation of the wave spectrum based on only the absolute values of the transfer functions, i.e. only considering the spectra of  $\chi \in [0 \ 180]$  deg.  $\beta_0$  is chosen based on the angle where the lowest variation occurs which is indicated by the vertical dotted line, the significant wave height is taken as the average value of the responses at the same angle.

The information retrieved from the first estimate, which can be seen in Fig. 7, is not enough since it only indicates the heading on the spectrum of  $\chi \in [0 \ 180]$  and the intention is to calculate on the full compass,  $\chi \in [0 \ 360[$  deg. To do so, the imaginary parts of the transfer functions must be included in the estimation. Two examples of the results of this practice are shown in Fig. 8 where the actual wave heading estimate is found where the blue line, named 'Total', takes its minimum value. This secondary heading estimate is  $\beta_2 \in [0 \ 360]$  deg. From Fig. 9-10, the second estimated heading  $\beta_2$ , based on the imaginary parts of the transfer functions, i.e.

considering the whole spectra of  $\chi \in [0 \ 360[$  deg., and gives the heading as the position where the 'Total' line takes the minimum value which is indicated with the vertical dotted line. The generated information about the wave is in the encounter wave domain and must be transformed in to the absolute domain which is carried out by using the information about the wave spectrum itself. By using the information about the wave angle and the vessel speed, it is possible to know the characteristics to calculate the absolute domain spectrum by introducing the Doppler effect. After doing so, all the information wanted is estimated, which implies values on the significant wave height, the wave encounter angle and the periods.

The result of the described procedure, to investigate how well the transfer functions performs compared to the reality, can be seen in Fig. 11. In Fig.11a it is possible to see the measured wave spectrum together with a parametric wave-spectrum according to Bretschneider theory. The comparison shows a good correlation which means that the given wave parameters describe the wave oceans in a fairly good way, indicating that the data of the wave spectrum is correct. In Figs. 11(b-d) the comparison between the measured motions and the re-calculated motions using the transfer functions can be seen and it is clear that there is a difference between the two-response spectrums for each motion. This indicates that either the measured motions and/or the transfer functions are faulty. In an effort to trace if the error originated in the transfer functions or in the measured responses, one more comparison was done with a new set of transfer functions received from DNVGL with similar errors as shown in Fig. 11.

The overall observation from the study implies that speed influences the performance of a drillship in the encounter domain and does not align with measured values. The realities of the ocean waves truly influence how well drillship may perform, and it is crucial to know that the actual performance may deviate from the measured values due to the condition of the sea.

## 5. Conclusion

The study revealed the disparities in measured and simulation results as applied to the seakeeping ability of a drill ship. The wave height and true heading state was observed to be higher in the simulation results compared to the numerical results (measured values). Also, the accuracy of the estimation of the peak period has been shown to be relatively high while the accuracy for the mean period and zero-up crossing period deviated from the true value. In view of the study findings, measured values are not reflections of the true heading state of a drillship, as there is need for incorporating more modified systems and simulations to predict a ship keeping ability under various wave impacts at sea.

## References

- Chen, Q., Lau, Y., Zhang, P., Wang, T.N., & Wang, N. (2023). Unmanned vessel research in China, *Heliyon*, 02, 13-19.
- Daiyong, Z., Xiumin, C., Chenguang, L., Zhibo, H., & Wenxiang, W. (2024). A Review on Motion Prediction for intelligent Ship Navigation, *J. Mar. Sci. Eng*, 12(1), 1-34
- De-Alwis, M.P, LoMartire, R., Ang, B.O Garne, K. (2020). Exposure aboard high performance marine craft increases musculoskeletal pain and lowers contemporary work capacity of the occupants, proceedings of the Institution of Mechanical Engineers, *Journal of Engineering for the Maritime Environment*, 235,750-762.
- Eliopoulou, E., Alissafaki, A., & Papanikolaou, A. (2023). Statistical Analysis of Accidents and Review of Safety Level of Passenger Ships, *Journal of Maritime Science*, 11, 400-412.
- Karol, D., CO. & Young, I.R (2020). On the measurement of directional wave spectra, *applied ocean research*, 16, 283-294.
- Marion, Z., Karl, G., Anders, R. (2024). Seakeeping criteria revisited, *Ocean Engineering*, 297, 3933-3991.

- NATO, (2018). Common procedures for seakeeping in the ship design process, *Journal of ocean Engineering and Science*, 7, 34-48.
- Nielsen, U.D., Astrid, H.B., Asgeir, J.S. (2018). A brute-force spectral approach for wave estimation using measured vessel motions, *marine structures*, 60, 101-121.
- Romero-Tello, P., Guti, J. E., & Sern-Camas, B. (2023). Prediction of sea keeping in the early stage of conventional mono-hull vessels design using artificial neural network, *Journal of ocean Engineering and Science*, 8, 344-366.
- Subhdeep, G. (2022). What does seakeeping of vessels mean? *Naval architecture, Ocean*, 3(2), 16615-16629. [www.marineinsight.com](http://www.marineinsight.com)
- Volker, B. (2012). *Practical Ship Hydrodynamics*, 2<sup>nd</sup> edition, 12(1),.123-141.